

---

This is an electronic reprint of the original article.

This reprint may differ from the original in pagination and typographic detail.

Taebnia, Mehdi; Toomla, Sander; Leppä, Lauri; Kurnitski, Jarek

## Air Distribution and Air Handling Unit Configuration Effects on Energy Performance in an Air-Heated Ice Rink Arena

*Published in:*  
Energies

*DOI:*  
[10.3390/en12040693](https://doi.org/10.3390/en12040693)

Published: 20/02/2019


*Document Version*  
Publisher's PDF, also known as Version of record

*Published under the following license:*  
CC BY

*Please cite the original version:*  
Taebnia, M., Toomla, S., Leppä, L., & Kurnitski, J. (2019). Air Distribution and Air Handling Unit Configuration Effects on Energy Performance in an Air-Heated Ice Rink Arena. *Energies*, 12(4), Article 693.  
<https://doi.org/10.3390/en12040693>

## Article

# Air Distribution and Air Handling Unit Configuration Effects on Energy Performance in an Air-Heated Ice Rink Arena

Mehdi Taebnia <sup>1,\*</sup>, Sander Toomla <sup>2</sup>, Lauri Leppä <sup>3</sup> and Jarek Kurnitski <sup>1,4</sup> 

<sup>1</sup> Aalto University, Department of Civil Engineering, P.O. Box 12100, 00076 Aalto, Finland; jarek.kurnitski@aalto.fi or jarek.kurnitski@taltech.ee

<sup>2</sup> Granlund Consulting Oy, Malminkaari 21, PL 59, 00701 Helsinki, Finland; sander.toomla@granlund.fi

<sup>3</sup> Leanheat Oy, Hiomotie 10, FI-00380 Helsinki, Finland; lauri.leppa@leanheat.fi

<sup>4</sup> Department of Civil Engineering and Architecture, Tallinn University of Technology, Ehitajate tee 5, 19086 Tallinn, Estonia

\* Correspondence: mehdi.taebnia@aalto.fi

Received: 14 January 2019; Accepted: 15 February 2019; Published: 21 February 2019



**Abstract:** Indoor ice rink arenas are among the foremost consumers of energy within building sector due to their exclusive indoor conditions. A single ice rink arena may consume energy of up to 3500 MWh annually, indicating the potential for energy saving. The cooling effect of the ice pad, which is the main source for heat loss, causes a vertical indoor air temperature gradient. The objective of the present study is twofold: (i) to study vertical temperature stratification of indoor air, and how it impacts on heat load toward the ice pad; (ii) to investigate the energy performance of air handling units (AHU), as well as the effects of various AHU layouts on ice rinks' energy consumption. To this end, six AHU configurations with different air-distribution solutions are presented, based on existing arenas in Finland. The results of the study verify that cooling energy demand can significantly be reduced by 38 percent if indoor temperature gradient approaches 1 °C/m. This is implemented through air distribution solutions. Moreover, the cooling energy demand for dehumidification is decreased to 59.5 percent through precisely planning the AHU layout, particularly at the cooling coil and heat recovery sections. The study reveals that a more customized air distribution results in less stratified indoor air temperature.

**Keywords:** ice rinks; air distribution solutions; indoor air temperature gradient; air handling unit configuration; building energy efficiency; building performance simulation; energy and HVAC-systems in buildings

## 1. Introduction

The reduction of energy use in buildings is a strategic research challenge, due to the significant contribution of the building sector in CO<sub>2</sub> emissions. The reduction of energy use and the improvement in energy efficiency is strongly linked to the operations and performance of passive and active systems in buildings [1]. The potential for the reduction of energy demand has to be evaluated through the prioritizing solutions based on their energy efficiency [2]. Specifically, indoor ice arenas among the building sector are an enormous consumer of energy, due to their unique indoor conditions. The yearly energy consumption of a standard single ice rink arena is typically estimated to be between 1000–1500 MWh [3,4]. However, the range of individually measured energy consumptions is even larger, within 500–3500 MWh/year, which provides a great potential for energy savings [5]. The ice pad refrigeration and hall space heating are two major contributors to the energy use of the ice rinks. By default, to maintain a steady-state condition, the heat removed from the hall primarily by the

refrigeration machinery needs to be roughly matched with the heat supplied into and generated inside the hall. In the case of an air-heated arena, the vast majority of the heat balance is maintained through a heated supply of air.

Generally, ventilation efficiency in similar sports halls such as swimming pools could potentially be improved by various alternative air distribution concepts [6]. However, the unique indoor conditions of an ice rink arena proposes challenges to energy-efficient heating and ventilation. Due to the cooling effect of the ice pad, a vertical temperature gradient inside the hall space is unavoidably formed. This, accompanied with the fact that the recreational activities practiced on the ice pad require a free height of approximately five meters, makes space heating of the rink difficult. In fact, in order to maintain a set temperature at an occupational height above the ice pad, the temperature of the supply air entering the hall at a height below the ceiling has to exceed the occupational set point temperature by a large amount.

Several past studies have focused on reducing the heat load towards the ice pad, and thereby reducing the refrigeration unit's electricity consumption [7–9]. Simultaneously, numerous efforts have gone into modeling the air distribution inside the hall space in experimental, zonal model, or Computational Fluid Dynamics (CFD) form [10–14]. As a result, we have a fairly comprehensive understanding of the temperature and moisture profiles inside the hall, as well as the factors affecting the heat load.

The vertical distribution of temperature in various ice rinks has been measured in current and previous studies [12,14–17] and their outcome as temperature gradient curves is used in this paper, while similar ice rinks as case study arenas have been measured.

However, the actual role of the air handling unit (AHU), along with its components and control strategies, has only been briefly investigated in two prior publications. Seghouani [8] modeled the AHU of a simulated ice arena hall space as a two-speed system, either low or high, which is increased to high-speed mode only during ice pad resurfacing, to evacuate the combustion gases of the resurfacing vehicle, with no air recirculation or no extract air heat recovery [8]. Piché [18] continued Seghouani's research by adding two possible modifications to the AHU modeled earlier: an alternative pre-heated fresh air source, or an air-to-air heat exchanger, both of which utilized the refrigeration unit's condenser heat. While the later study obtained significant results regarding the AHU's energy demand compared to the prior one, neither implementations represented a typical, modern, real-life indoor ice rink AHU solution. This means that previous studies about AHUs are outdated, and they do not represent a modern AHU layout. Thus, the energy performance of modern AHUs, equipped with full variable-air-volume (VAV) control, a heat exchanger (HX) for extract air heat recovery, and the possibility for extract air recirculation, in the context of demanding indoor ice rink conditions, should be further investigated.

The objective is to determine (quantify) the impacts of indoor temperature stratification, as well as AHU layouts, on energy consumption, while two commonly used AHU configurations at different temperature gradients are applied. To study the two focus features, the AHU design, and the air stratification intensity, we present six simulation setups, which are based on existing ice rink arenas in Finland.

The AHU for the hall space of an air-heated ice arena usually has three main objectives. Firstly, as with any ventilation system, it should provide adequate fresh air into the space, to maintain satisfactory indoor air conditions. Secondly, in this case, it is solely responsible for supplying the space with enough heat. Thirdly, in case, no external dehumidification equipment is present, and the AHU is equipped with a condensing dehumidifier, and it is thus responsible for maintaining the moisture content under a specific set point inside the hall. The indoor air recirculation is implemented by the maximum possible rate at any moment, for energy conservation. Each AHU has its own theoretical energy demand, depending on its main objective. To maximize the AHU's energy efficiency, it should be demand-controlled, based on CO<sub>2</sub>, temperature, and humidity set point levels, depending on their measured values. If either of the measured values in a particular moment exceeds the acceptable

range, then that parameter's control signal prevails to other signals. In the case of simultaneous exceeding of set points, the automation system reacts simultaneously so that each parameter can react independently, by sending its control signal to the associated section of AHU to that parameter. Two air-handling layouts have been used as the simulation model in this study. A section of the air-handling units (AHU1.1) and (AHU2.1) are shown in Figure 1, and their specifications are described in the following paragraphs.

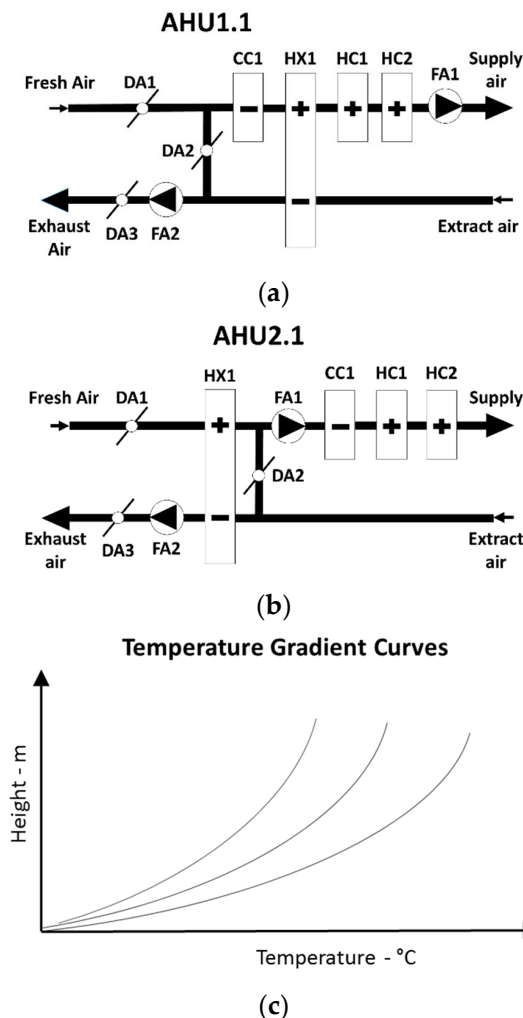


**Figure 1.** AHU layouts and temperature gradient curves. (a) Schematic view of AHU1.1; (b) Schematic view of AHU 2.1; (c) Estimated models for temperature gradients.

The air handling unit 1.1 (AHU1.1), depicted in Figure 1a, is fully automated, equipped with extract air recirculation, a cooling coil (CC) acting as a condensing dehumidifier, a rotary heat exchanger (HX) for extract air heat recovery, with an assumed efficiency of 85%, and two heating coils (HC). HC1 utilizes condenser heat from the refrigeration plant, while HC2 is connected to the district heating system. HC2 acts as a backup heat device in case the refrigeration unit is not operating or is not producing enough condenser heat. In the simulation, HC1 is not modeled. Both the supply and exhaust fans are fully VAV-compatible up to 4 m<sup>3</sup>/s, and their speeds are individually controlled. The exhaust fan is placed outside the recirculation loop, making it possible to recirculate air utilizing the supply fan only. The whole unit is demand-controlled based on temperature, humidity or CO<sub>2</sub>-level measurements from the ice rink.

AHU2.1, is in many aspects very similar to AHU1.1, except for one key difference. The rotary heat exchanger with an assumed efficiency of 85% is placed outside the recirculation loop, as presented

in Figure 1b, leaving it completely unavailable for recirculation mode. The supply and extract fans are demand-controlled in the same fashion as AHU1.1 and rated up to 4 m<sup>3</sup>/s. Supply air is cooled and dehumidified with a condensing dehumidifier. It is then heated with two heating coils. The HC1 utilizes condenser heat and the HC2 district heat, similar to AHU 1.

In this study, we concentrate first on the AHU design and its control approach, by presenting two AHU layouts that only differ from the position of their heat exchangers. Second, we study the temperature stratification of indoor air and its effects on energy consumption in a simplified way. We also study how various air distribution designs relate to a temperature gradient. The air stratification intensity of the cases is based on real measured data in three ice rink arenas, similar to a previous study [14]. Overall, six cases are presented for the simulations, two AHU layouts, and three temperature gradients. The results of on-site measurements can only verify three of these cases, since each ice rink is equipped with only one of the AHUs.

There are three ice rink arenas, each with a demand-controlled AHU equipped with a condensing dehumidifier. However, their final implementations regarding components and control strategies differ from each other. In this publication, six simulation models are presented for the ice rinks, similar to the real-case study rinks, and their measured data have been used to verify the simulation results. The heating and cooling energy demands for each AHU, along with the indoor air conditions, as well as their temperature stratifications, are also presented.

## 2. Methods

### 2.1. Buildings and Air Handling Units

The three indoor air distribution models selected for use in this study are presented in Figure 2. The reasons for selecting these particular models is firstly, because they are existing ice arenas in Finland, and second, because both the required measurements for this study (temperature gradient and energy consumption measurements) were implemented there. This means that each of the indoor air distribution models corresponds to one of the measured temperature gradients. Therefore, these selected air distribution models were the case study models.

The rather simple air distribution system corresponding to the measured temperature gradient of 2.1 is depicted as the hall space cross-section in Figure 2a. The supply air terminals of this system are located below the ceiling level, and their air jets blow horizontally to the opposite directions. The extract air terminal is located close to one end along the space.

The air distribution system corresponding to the temperature gradient of 1.6 consists of multiple supply air terminals located above the spectator balcony, angled towards the ice pad. A cross section of the hall space is depicted in Figure 2b. Supply air jets are located along the length of the hall, while extract air is drawn from terminals located near the end alongside the hall. In the vertical direction, both the supply and extract terminals are close to the ceiling level.

The air distribution system corresponding to a temperature gradient of 1.5 is unlike the other presented systems. Non-heated supply air enters the hall space from terminals connected to small holes drilled to the sideboards of the rink. The idea is to ventilate the occupational zone above the rink without compromising the quality of the ice pad with heated air. Heated supply air is distributed at an angle towards the stands, while the extract air terminal is located towards the end of the hall below the ceiling. The system is presented in Figure 2c.

To verify the simulation results we used the experimental data from real ice arenas. It is important to present the unique features of each arena. This generates errors that might favor some outcomes. If the results do not make sense without modification, we can then modify the simulations based on the unique features of the ice arenas, which have been experimentally measured. We would need to show that the differences in the simulations are also seen in the experimental measurements.

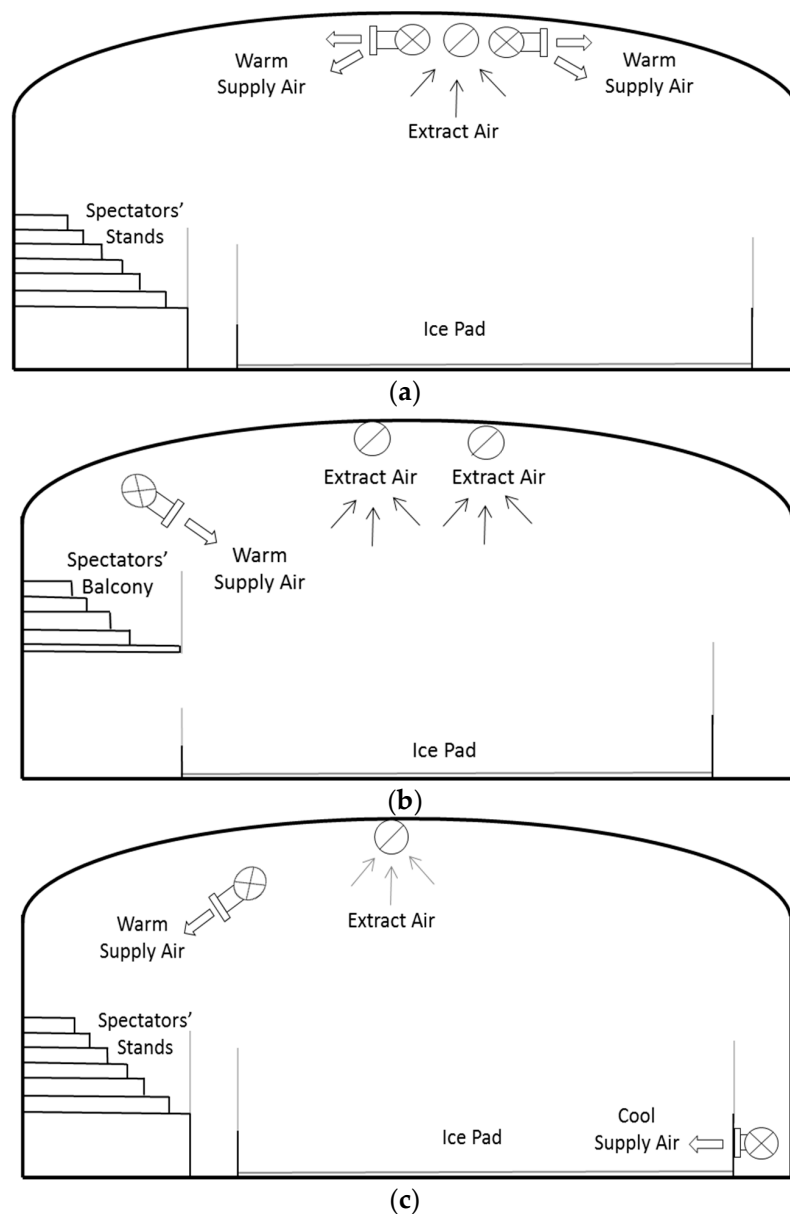


**Figure 2.** Air distributions corresponding to the measured temperature gradients: (a) A; (b) B; (c) C.

In order to compare the AHUs' performance against outdoor and indoor conditions, a series of measurements were performed. A Temperature and relative humidity (T/RH)-logger, shielded with direct insolation, was used to track the temperature and relative humidity of the outdoor air in close proximity of the studied building. Inside the hall space, T/RH/CO<sub>2</sub>-loggers measured the temperature, relative humidity, and CO<sub>2</sub> level of the indoor air, both from the skater's occupational zone above the ice rink, and from the stands. Due to practical reasons, the logger measuring the skating zone was placed just outside the rink at a height of 2 to 2.5 m above the rink, depending on the case.

The case study for this publication included four similar single ice rink indoor arenas, built between 2003 and 2015, located in the southern parts of Finland. Their ice pad sizes ranged from 1456 m<sup>2</sup> to 1566 m<sup>2</sup> (56 ... 58 × 26 ... 27 m<sup>2</sup>), with the arena hall volumes falling between 13,000 m<sup>3</sup> and 16,000 m<sup>3</sup>. The smallest arena had an elevated spectator balcony with the capacity for 60 standing spectators, while the others had stands rated for 500 to 750 seated spectators. Other spaces in the studied ice rink facilities were not considered in this publication. The descriptions for each measured AHU and their air distribution systems are as follows.

The air distribution system corresponding to AHU 1.1 is a combination of the air distribution system as shown in Figure 2b, and the AHU1.1 which is depicted in the following Figure 3.

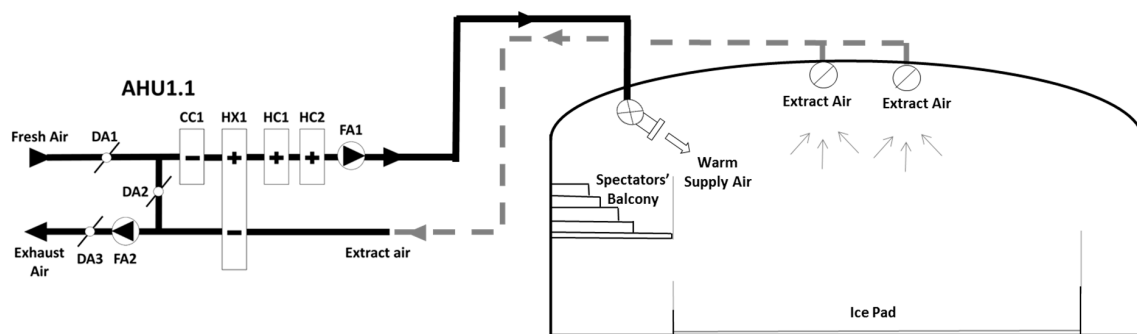


Figure 3. Schematic view of AHU1.1 and its corresponding air distribution.

AHU1.2, presented in Figure 4, is similar to AHU1.1, which is presented earlier with some modifications. The demand control strategy, based on the temperature, humidity or CO<sub>2</sub> level, is the same as the order of components in the supply side of the unit (recirculation to cooling coil, heat exchanger, and to the heating coils). The core differences are:

- Supply air is split into a heated and non-heated flow. The HC for the heated supply air utilizes condenser heat from the refrigeration plant, while the only form of heating for the non-heated air is extract air heat recovery.
- The extract air heat recovery unit is a cross-flow air-to-air plate heat exchanger instead of a rotary heat exchanger, as in AHU1.1
- The supply and exhaust fans are rated up to 5 m<sup>3</sup>/s correspond to 2.5 L/sm<sup>2</sup>.
- The exhaust/extract fan is located inside the recirculation loop; in full recirculation mode, both fans need to be operated.

In the hall space, the heated supply air is directed towards the stands and outside the rink, while the non-heated portion serves as ventilation for the ice pad area. The extract air terminal is located below the ceiling level approximately in the center of the space. A cross-section of the space, along with the air distribution arrangement, can be examined in Figure 4.

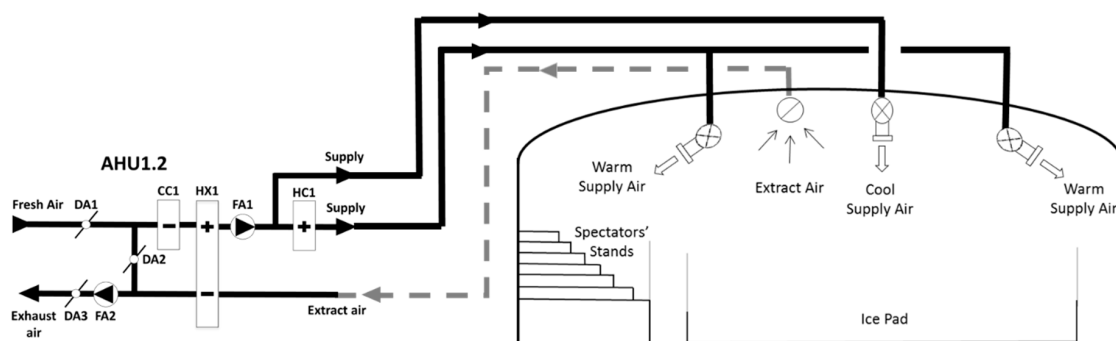


Figure 4. Schematic view of AHU1.2 and its corresponding air distribution system.

AHU2.2 differs from the other presented units in that it is not fully VAV-compatible. It is operated as a two-speed unit, namely half- and full-speed, but both speed options can be programmed to any percentage of the fan's maximum capacity. The supply fan is rated up to 4 m<sup>3</sup>/s, and the exhaust fan up to 2 m<sup>3</sup>/s. Like AHU1.2, the unit is equipped with regenerative exhaust air heat recovery outside the recirculation loop, and like AHU1.2, the supply air is split into heated and non-heated airflows. The non-heated flow is untreated after the condensing dehumidifier, making its temperature lower



than in AHU2.1. The heating coil utilizes condenser heat from the refrigeration plant. A schematic view of AHU2.2 is available in Figure 5.

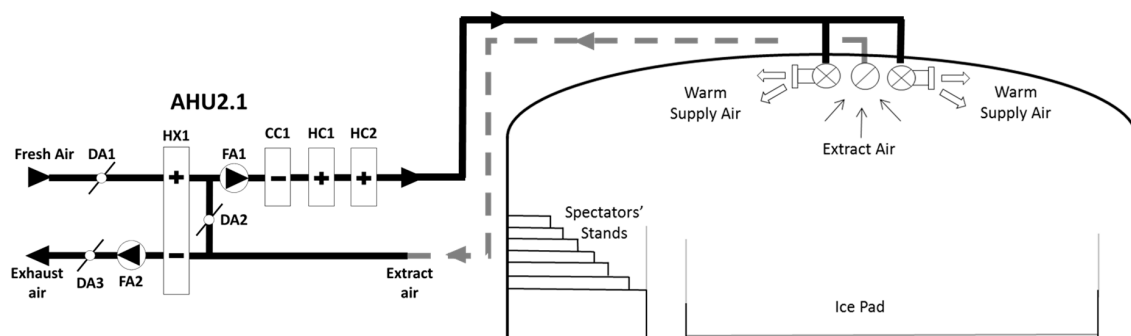


Figure 5. Schematic view of AHU2.1 and its corresponding air distribution system.

The air distribution system corresponding to AHU2.2 is unlike the other presented systems. Non-heated supply air enters the hall space from terminals connected to small holes drilled to the sideboards of the rink. The idea is to ventilate the occupational zone above the rink without compromising the quality of the ice pad with heated air. Heated supply air is distributed at an angle towards the stands, while the extract air terminal is located towards the end of the hall below the ceiling. The system is presented in Figure 6.

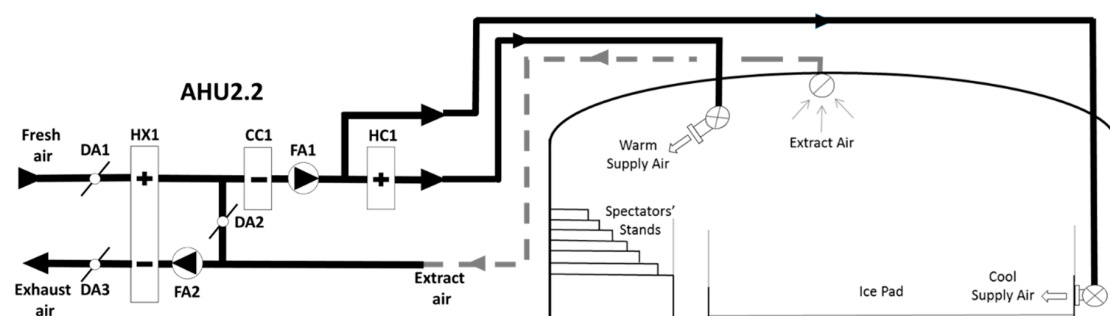


Figure 6. Schematic view of AHU2.2 and its corresponding air distribution system.

It is important to explain that the four models described above are used for 24 h measurements, but there are temperature gradients measured in only three of them. Therefore, those three, which are similar, as shown in Figure 2a–c, were used to validate the simulation results.

## 2.2. Measurements

For each AHU and its corresponding hall space, a series of measurements were carried out. The measurement periods lasted between six and eight days, and the measurement interval was five minutes. The measurement plan of each AHU could not be perfectly implemented, due to differences in the air handling units' space coverage, capacity, and accessibility to the measurement locations. The missing measurements were compensated with measurements performed from the building automation system, when possible. All of the measurements were carried out within May and June 2016.

The indoor air temperature and relative humidity were measured and logged with T/RH-loggers (THERMADATA MALLI) before and after each AHU component, i.e., before and after the heating coils, the cooling coils, and the heat exchangers. The indoor air CO<sub>2</sub> levels were measured with T/RH/CO<sub>2</sub>-loggers at the supply and extract air or extracted air positions. Meanwhile, fresh air was assumed to have a constant CO<sub>2</sub> level of 400 ppm. For airflow rates, the pressure difference over the fan was measured and logged, and it could then be converted into an airflow rate by using a



unit-specific k-factor. An overview of the conducted measurements for each AHU is presented in Table 1.

**Table 1.** Overview of the conducted measurements. M = measured, M\* = measured short-term, AS = measured by the automation system, E = estimated, C = calculated, - = not valid for said AHU.

Measured Parameters		Airflows				Temperature and RH Change over:					CO <sub>2</sub> Level		
Measured at the Section	Fresh	Supply			Extract	Exhaust	CC	HC1	HC2	HX	Fresh	Supply	Extract
		Total	Heated	Non-Heated									
Machines													
AHU 1.1	C	M	-	-	E	M	M	M	M	M	E	M	M
AHU 2.1	C	M	E	E	M	C	M	M	-	M	E	M	M
AHU 1.2	C	E	-	-	E	C	M	M	M	M	E	M	M
AHU 2.2	C	M	C	M*	E	C	M	M/AS	-	M	E	M	M

As Table 1 states, a series of estimations had to be made, especially regarding the airflow rates. When the extract airflow could not be measured, due to the fan's location or the lack of available pressure differential measuring points, the extract airflow rate was estimated to match the supply airflow rate. For AHU 1.2, the airflow measurements could not be performed at all without interfering with the unit's operation. However, examining the temperature and RH changes in the supply air made it clear the unit was operated in an on-off fashion. For example, the temperature of the supply air after the cooling coil would periodically lower to a constant value for a while, and then rise to another value that was constant along the whole unit. Based on this behavior, it could be estimated that the air inside the unit was partially moving and partially standing still. For when the air was moving, it was estimated that the unit worked at full capacity, and when the air was evidently standing still, the airflow rate was set to 0 m<sup>3</sup>/s. The resulting average airflow rate was in line with measured average rates from the other AHUs.

For AHU 2.1, as the ratio between the heated and non-heated supply airflows could not be experimentally determined, and the flow rates were estimated at 80% and 20% of the total supply airflow, respectively. The estimated ratio resulted in a total supply air average temperature that was in line with the produced thermal conditions inside the hall space. For AHU2.2, the flow rate of the non-heated supply air was determined in short-term measurements, and the calculated ratio between the heated and non-heated supply flows was estimated to stay constant throughout the measurement period.

### 3. Simulation Setup and Building Model

To highlight the core differences between the studied AHUs, and to exclude any external variables affecting their performance, a version of each AHU was modeled, and its performance was simulated by using IDA ICE v. 4.7.1 with the Ice Rinks and Pools 0.912 add-on, for a period of one year, with typical meteorological conditions for Helsinki, Finland. The simulated demand-control-strategy, based on temperature, relative humidity, and CO<sub>2</sub>-measurements from the hall space, was unmodified across the modeled AHUs. Three of the built simulation models were validated by using experimental data. For comparison's sake, Seghouani presented, modeled and simulated a modified VAV-version of the AHU to study its performance [8].

#### 3.1. Building Specifications

We used a rather simplified approach that was common to all simulation models. We used a one-zone airspace with a size of 65 × 35 × 7 m, and one door with a size of 3.5 × 5.0 m, which was opened seven times a day for 10 min each time. The external walls of the building were made of Aluminum 0.003 m, light insulation 0.2 m and aluminum 0.003 m. The Roof was made of Aluminum 0.003 m, light insulation 0.3 m, and renders 0.01 m. The external floor was made of floor coating 0.05 m

and 0.2 m concrete. The main door was made of 0.003 m aluminum. There were no thermal bridges formed in the building. Infiltration through the building was constant, with 0.03 ACH.

The cooling pipes were submerged 2 cm into the concrete slab underneath the ice pad. The rest of the 0.2 m concrete slab and an insulation layer of 0.1 m formed the base layer underneath the ice pad. Heating pipes are located in the soil beneath the insulation layer. The cooling and heating powers were  $200 \text{ W/m}^2$  and  $40 \text{ W/m}^2$ , respectively. The ice layer thickness was 3.5 cm, and the ice temperature set-point was  $-5 \text{ }^\circ\text{C}$ .

### 3.2. Control Strategy

The zone was ventilated and heated by the AHU, which was controlled based on the measured indoor and extract air conditions. The AHU maximizes the recirculation air usage for energy conservation. The supply and the exhaust fans were controlled by responding to the measured temperature, relative humidity and  $\text{CO}_2$  values of the zone, with boundaries of  $4\text{--}6 \text{ }^\circ\text{C}$  (corresponding to output signals of either 1 or 0 respectively), 60–70% RH and 1000–1100 ppm  $\text{CO}_2$  (both corresponding to outputs of 0 and 1, respectively). The supply air temperature was adjusted according to the zone average temperature with simplified set points of  $30 \text{ }^\circ\text{C}$  when the indoor air temperature was below  $3 \text{ }^\circ\text{C}$ , and  $3 \text{ }^\circ\text{C}$  when the air temperature was above  $7 \text{ }^\circ\text{C}$  (Figure 4). The heat recovery unit was always on. The cooling coil cooled and dehumidified by reducing the air temperature to  $+1 \text{ }^\circ\text{C}$  when the moisture content of the air exceeded  $3.65 \text{ g/kg}$  dry air. The fresh air intake was controlled by the  $\text{CO}_2$  concentration of the extract air, according to a setpoint range of 1000–1100 ppm, corresponding to outputs of 0.037 and 1, respectively. The minimum fresh air intake was set to 3.7%, as reported by Toomla [14]. The extract air  $\text{CO}_2$  concentration with set points of 1000–1100 ppm, corresponded to signals of 0 to 1, respectively. The  $\text{CO}_2$  concentration of extract air controlled the exhaust fan as well. Both fans were rated up to  $4 \text{ m}^3/\text{s}$  ( $2.0 \text{ L/s/m}^2$ ) capacity, according to ASHRAE 90.1, with the Specific Fan Power (SFP) set to  $1.23 \text{ (kW/m}^3/\text{s)}$ , and the efficiency to 0.6.

### 3.3. Assumptions and Parameters for the Simulation Models

The supply fan was operated based on the zone signal. Smooth functions (from 0 to 1) for high-temperature HI 6 and low-temperature LO 4, RH HI 0.7 LO 0.6,  $\text{CO}_2$  HI 1100 LO 1000, and MAX signals of these three controlled the supply fan speed. The exhaust fan was controlled by the  $\text{CO}_2$  content in the extract air. A smooth function of 0 to 1 was set with HI 1100 and LO 1050, i.e., therefore, the exhaust fan only ran when the  $\text{CO}_2$  level was high.

The recirculation of indoor air or outdoor air intake was controlled by the extract air  $\text{CO}_2$  content, with a smooth function 0.037 (3.7%) to 1 (100%), with LO 1000 and HI 1100.

Heat exchangers always function with an effectiveness of 0.85 and an unknown capacity. The minimum allowed leaving temperature was  $+1 \text{ }^\circ\text{C}$ . Drying with the cooling coil was controlled so that the temperature set point was the minimum from either the incoming temperature or the incoming humidity control, so that the cooling coil temperature set points were  $4 \text{ }^\circ\text{C}$  below  $3.15 \text{ g/kg}$ , and  $1 \text{ }^\circ\text{C}$  above  $3.65 \text{ g/kg}$ . The cooling coil effectiveness causes a liquid-side temperature rise of  $5 \text{ }^\circ\text{C}$ . The cooling was simulated as district cooling, to show the cooling demands of the dehumidification.

The heating coil effectiveness was 1, and the liquid-side temperature drop was  $20 \text{ }^\circ\text{C}$ . The heating coil set-point temperature for the supply air was controlled by the zone average air temperature, according to the curve presented in the Figure 7.

The indoor air temperature gradient was set, based on the three variants' measured values,  $1 \text{ }^\circ\text{C/m}$ ,  $1.5 \text{ }^\circ\text{C/m}$ , and  $2 \text{ }^\circ\text{C/m}$ .

Lighting was carried out with  $20 \times 400 \text{ W}$  ( $4.0 \text{ W/m}^2$ ) units with a luminous efficacy of  $12 \text{ lm/W}$ , and a convective fraction of 0.5. The lighting was used only when players were present. Inside the zone, there was an ice pad ( $60 \times 30 \text{ m}$ ) with Freezium as the coolant and heating medium.

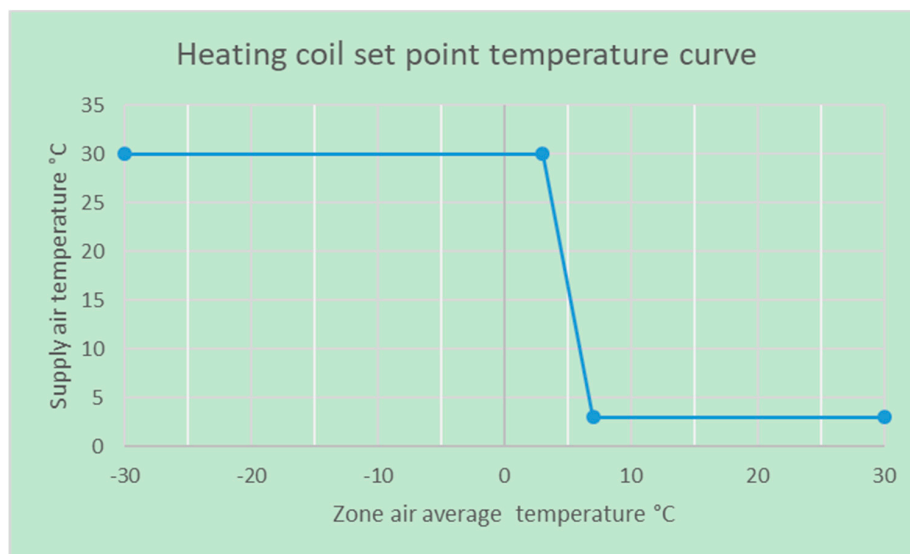


**Figure 7.** Heating coil set-point temperature curve to control the supply air.

Figures 8 and 9 are a few examples of how the system and control set-points were set in the simulation software. All of the properties of the system were simply set in the IDA-ICE simulation software, as shown in the Figure 8, where the operation set points of the refrigeration plant, the ice pad, subfloor heating, and further details were set. The indoor air control set-points (air flow, temperature, relative humidity) were also set in the IDA-ICE (4.7.1, EQUA, Stockholm, Sweden), as shown in Figure 9.

Cooling		Subfloor heating	
Secondary coolant	Freezium	Medium	Freezium
Freezing point	-35 Deg-C	Freezing point	-35 Deg-C
<b>Cooling supply line</b>		<b>Heating supply line</b>	
Length	40 m	Length	40 m
Inner diameter	0.1 m	Inner diameter	0.05 m
<b>Parallel cooling coils</b>		<b>Parallel heating coils</b>	
Pipe level below ice bottom	0.02 m	Pipe level below ice bottom	0.37 m
number of coils	100	number of coils	20
length per coil	40 m	length per coil	40 m
Inner diameter	0.025 m	Inner diameter	0.025 m
<b>Freezing operating point</b>		<b>Subfloor operating point</b>	
Cooling power	200 W/m2	Heating power	40 W/m2
Supply coolant temperature	-10 Deg-C	Supply temperature	10 Deg-C
Return temperature	-3 Deg-C	Return temperature	3 Deg-C
<b>Pump</b>		<b>Pump</b>	
Efficiency	0.8	Efficiency	0.8
Max pressure head	3000.0 Pa	Max pressure head	3000.0 Pa
<b>Coolant control</b>		<b>Medium control</b>	
Sensed temperature	Ice	Temperature setpoint	0 Deg-C
Temperature setpoint	-5 Deg-C		
Ice layer thickness	0.035 m	Pump energy meter	Rink Distribution Pumps

**Figure 8.** Refrigeration plant and the ice pad set points.

Control Setpoints			
	Min	Max	
Temperature	-15	30	*C
Mech. supply air flow	0	1.76	L/(s.m2)
Mech. return air flow	0	1.76	L/(s.m2)
Relative humidity	60	70	%
Level of CO2	800	1200	ppm (vol)
Daylight at workplace	100	10000	Lux
Pressure diff. envelope	-20	20	Pa

Figure 9. Indoor air ventilation quantity and quality setpoints.

The internal gains of the zone were the players, spectators, and lighting. The internal load of the players was set based on 20 players with an activity level of 5 Metabolic Equivalent of Task (MET), and scheduled as presented in Figure 10. On weekdays, the players were present from 7:00 to 9:00 a.m., and also from 3:00 to 10:00 p.m. On weekends, they were present from 9:00 a.m. to 9:00 p.m.

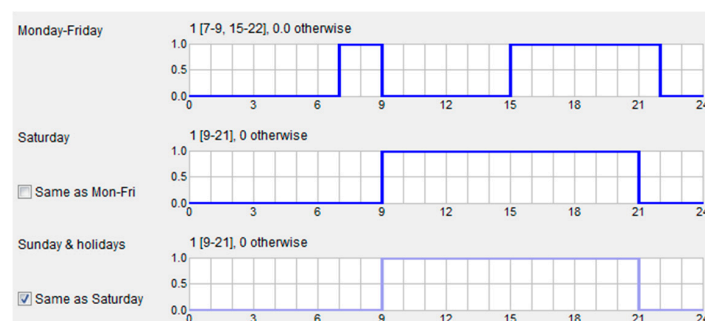


Figure 10. Scheduled internal loads of players.

Players were present according to the following schedule. The players' heat load was 20, with an activity level of 5 MET according to the schedule below, a maximum of 100 spectators, and  $20 \times 400$  W lamps.

The spectator attendance was modeled as 25 persons from 6:00 to 9:00 p.m. on weekdays, and as 50 persons from 9:00 a.m. to 9:00 p.m. on weekends, with a peak of 100 persons between 4:00 and 7:00 p.m.

The heat load caused by the spectators was set based on a maximum of 100 spectators, with an activity rate of 1.5 MET. The X factor, which is the percentage of spectators' occupancy in different days/times was implemented in the simulation according to the schedule presented in the following Figure 11:

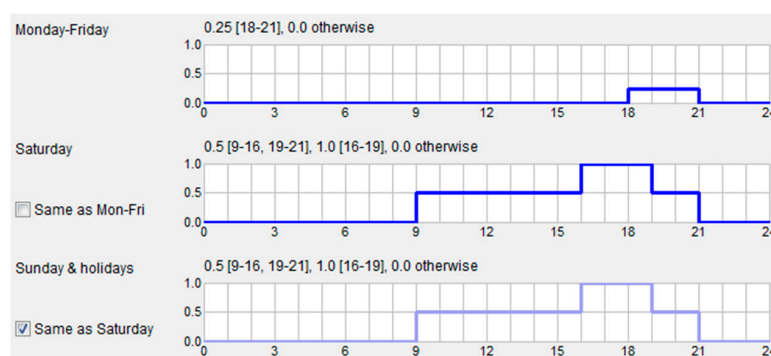


Figure 11. Scheduled internal loads of spectators.

The heat load of lighting with  $20 \times 400$  W lamps with a convective fraction of 0.5, was similar as player's schedule.

Finally, the temperature gradient values for the simulation models were set as  $2.0\text{ }^{\circ}\text{C}/\text{m}$  and  $1.5\text{ }^{\circ}\text{C}/\text{m}$ , to represent the average ice arenas, similar to the measured air stratification in real cases. In addition, the stratification value of  $1\text{ }^{\circ}\text{C}/\text{m}$  was set to describe an arena with a lower indoor air temperature gradient as an ultimate condition, which would be a significant improvement in comparison to the currently measured arenas.

### 3.4. Theoretical Heat Exchange and Airflow Principles

#### 3.4.1. Ice surface Modeling

In order to calculate the heat that is exchanged between the ice surface and the indoor air, we needed to concentrate on the transient model above the ice. To do so, it is initially required to determine the heat transfer coefficients of the air layer on the ice. Theoretical challenges on how accurate the model calculates the  $U_{\text{FILM}}$ , the  $H_{\text{CONV}}$ , and the condensation heat transfer through the ice surface to the hall space, are described as:

$$P_{in} = 10^5 \exp \left( 17.391 - \frac{6142.83}{273.15 + T_{in}} \right) \quad (1)$$

$$P_{ice} = 10^5 \exp \left( 17.391 - \frac{6142.83}{273.15 + T_s} \right) \quad (2)$$

The relative humidity at the height of  $h = 0.1$  m above the ice surface are calculated as follows:

$$RH_h = \left( \frac{h}{1.5} \right) \times (90 - RH_{1.5}) \quad (3)$$

$$dp = \left( \frac{RH_h}{100} \right) \times (p_h - p_{ice}) \quad (4)$$

$$dp_{atm} = \left( \frac{dp_{pa}}{101325} \right) \quad (5)$$

The heat transfer coefficient for condensation is also calculated as:

$$hd = 1750 \times h_{conv} \times \frac{\Delta P}{\Delta T} (RH_h/100) \quad (6)$$

$$q_{cond} = h_d \times (T_{in} - T_{ice}) \quad (7)$$

#### 3.4.2. Airflow Balance Equations

The calculated and measured airflow rates, along with the measured temperature and the RH changes over the components, were used to calculate the component theoretical energy output over the measurement periods. The heating powers of the heating coil and the heat exchanger were calculated as:

$$P_{heat} = q_{air} \rho_{air} c_{air} \Delta T_{air} \quad (8)$$

and the cooling coil's cooling powers as:

$$P_{cool} = q_{air} \rho_{air} \Delta h_{air} \quad (9)$$

where the enthalpy of air can be expressed as:

$$h_{air} = c_{air} T_{air} + x_{air} (c_w T_{air} + h_{we}) \quad (10)$$

The fresh air intake of the AHU was calculated based on CO<sub>2</sub>-level differences between the extract, supply, and fresh air. Any decrease in CO<sub>2</sub> level from the extract to supply air meant that a portion of the supply air was fresh air, since it is reasonable to assume no other CO<sub>2</sub> sources within the unit exist. Fresh air intake can be calculated as:

$$q_{fresh} = q_{sup} \left( \frac{C_{ext} - C_{sup}}{C_{ext} - C_{fresh}} \right) \quad (11)$$

The resulting flow rate for fresh air intake serves more as an approximation rather than an exact value, but its accuracy is sufficient to determine when the unit is operating in full or partial recirculation mode.

## 4. Experimental Results

### 4.1. Temperature Gradient Measurements

The vertical temperature profiles in various ice rinks in Finland were measured in previous studies [10–14], and its outcomes as temperature gradient curves are used in the current paper, as energy consumption of the same ice rinks has been measured to describe case arenas. The set air stratification intensity for the simulation is based on experimental measurements conducted in three ice rink arenas in Finland. The procedure of the measurements is subsequently described, and the measurement results are presented in Figure 12. The actual, non-linear temperature stratification was linearized into a gradient factor describing the temperature increase as degrees Celsius per meter. The cause for this simplification was the limitation of the simulation software.

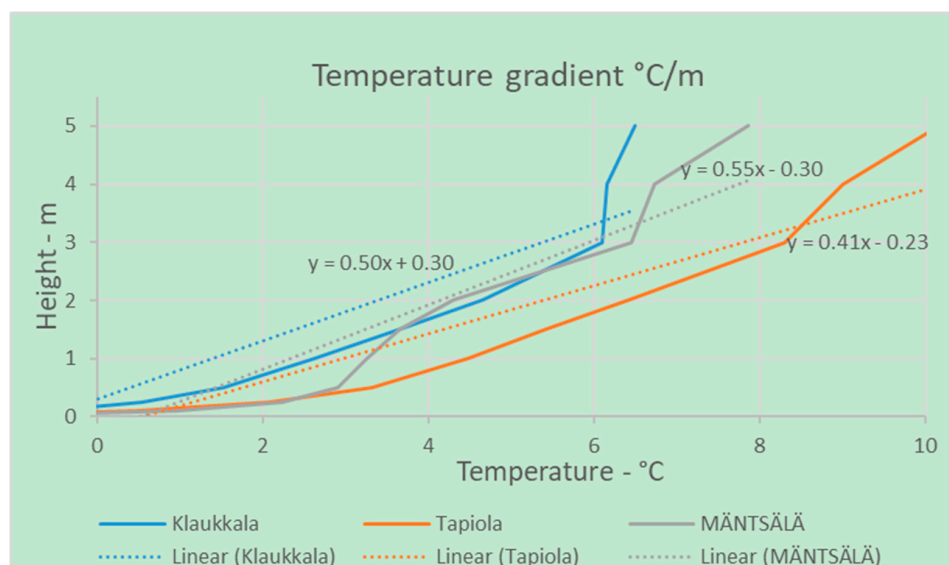


**Figure 12.** Air stratification measurement results of three ice arenas in Finland.

In order to understand the differences between the observed energy performances of each AHU, a perspective with regard to their respective outside air and produced indoor air conditions needed to be established. The 24-h periods of the AHUs were evaluated based on the maximum similarity of the outside air temperature and the hall space occupational load. It is noteworthy that neither the produced indoor air conditions nor the outside air humidity, which both affected the AHU's performance, were the same across the studied arenas. This limitation in the experimental setup will be taken into account when the results are discussed.

#### 4.2. The 24-h Outdoor and Indoor Air Measurements

The outside air temperature and relative humidity measurements were implemented for a selected 24-h period in close proximity to each case study arena, inside the arena hall space in the skating zone. The measurement results are presented in Figure 13a. The lower graphs always represent the temperature (left vertical axis) and the higher graphs represent the relative humidity (right vertical axis). The average temperatures were between 14.4 °C and 16.2 °C, while the average relative humidity has a larger range, 43.5% to 83.2%. The average indoor air temperatures were 3.5 °C to 8.8 °C, and the corresponding average relative humidity was 64.5% to 82%. Both are presented in Figure 13b. It is noteworthy that AHU1.2 produced the warmest and most humid conditions, even though temperature and relative humidity are inversely correlated with each other.

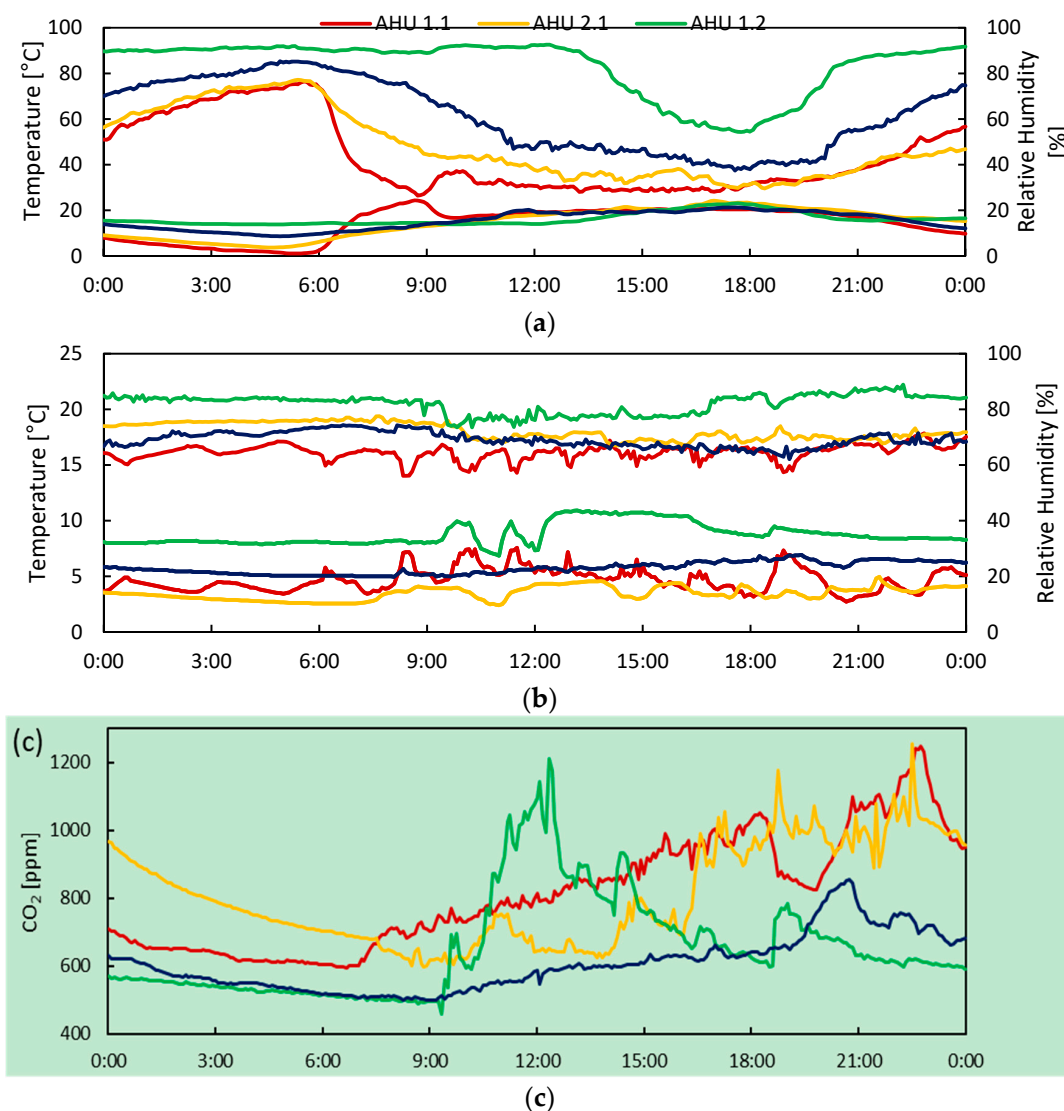


**Figure 13.** Indoor and outdoor air temperature, relative humidity and CO<sub>2</sub> measurements (a) Outside air temperature and relative humidity measurements; (b) Indoor air temperature and relative humidity measurements; (c) Indoor air CO<sub>2</sub> levels.

Hall space CO<sub>2</sub> levels are presented in Figure 13c. The CO<sub>2</sub> measurements are required to understand how indoor air CO<sub>2</sub> level changes against occupancy variations within a 24 h working period. It is particularly important to have a realistic perception about fresh air requirements, in order



to keep indoor air CO<sub>2</sub> levels in an acceptable range, which is necessary for the control settings of the simulation models.

AHUs 1.1, 2.1, and 2.2 followed an approximately similar air distribution system, where the indoor air CO<sub>2</sub> level more or less steadily increased towards the end of the day, while for AHU1.2, the peak was reached at midday. The calculated fresh air fraction of the supply air ranged from effectively 0% for AHUs 1.2 and 2.2, to 10% for AHU2.1 and 19% for AHU1.1. The fraction was observed to stay relatively constant for each AHU, regardless of the indoor air CO<sub>2</sub> level, leading to the conclusion that each AHU operated in what was set as its maximum allowed extract air recirculation rate.

#### 4.3. Energy Measurements at AHU Sections

The total external heating and cooling powers for each AHU are presented in Figure 14. The external power is defined as the power supplied to the supply air by the CCs and HCs. The heat exchanger was not considered, as it utilized internal heating power removed from the extract air. Heating power-wise, AHU 1.1 and 2.1 operated on a similar scale, with averages of 33 kW and 36 kW, respectively. AHU2.2 had a higher average of 45.3 kW, while the heating power of AHU1.2 was substantially larger, averaging at 81.3 kW. For the cooling power, the on-off type control of the CC of AHU2.2, as shown in 14b, led to the smallest average cooling power of 7.6 kW. The averages for AHU1.1, 2.1, and 1.2 were 13.6 kW, 25.6 kW, and 42.5 kW, respectively.

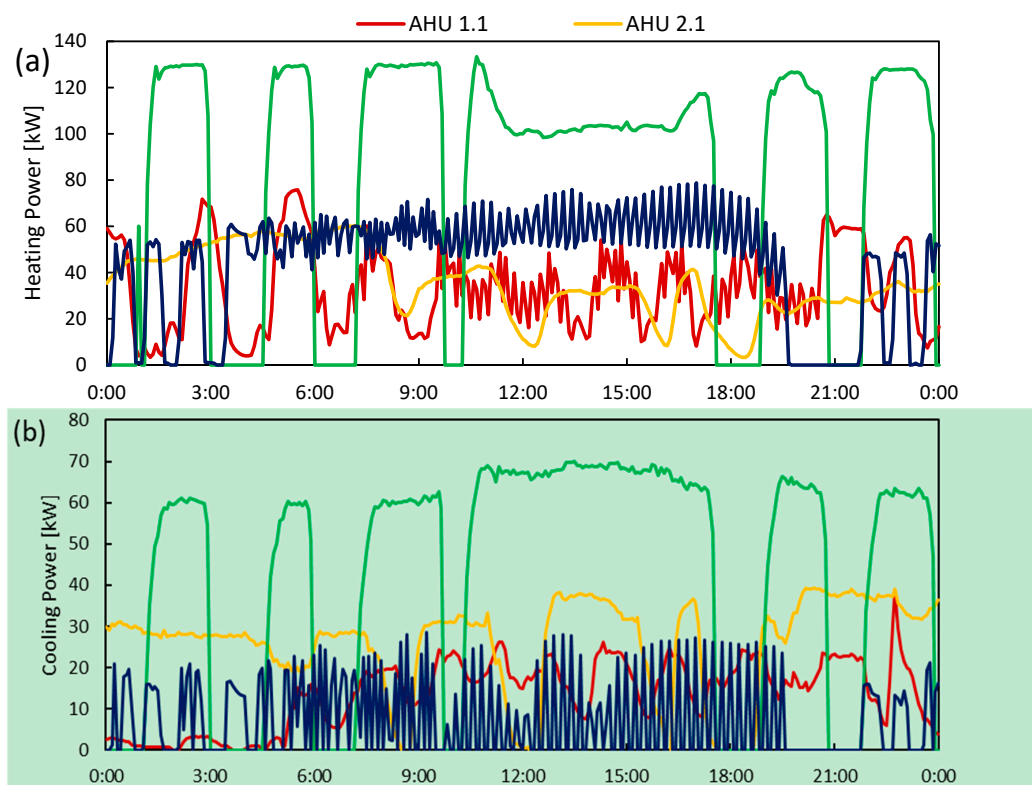


**Figure 14.** Total external (a) heating and (b) cooling power used by the AHUs for supply air treatment.

Figure 15 presents the total heating and cooling energy consumption by the supply air of the AHUs during the selected 24 h period, including heating energy supplied by the heat exchanger. Where the heat exchanger could be utilized despite the extract air recirculation, i.e., AHU 1.1 and 2.1, the heating energy supplied by the heat exchanger represented approximately 40% of the total heating energy demand. Total amounts of heating and cooling energy consumed by the supply air treatment ranged between 1088 kWh and 1951 kWh for heating, and between 182 kWh and 1021 kWh for cooling, as shown in Figure 15.

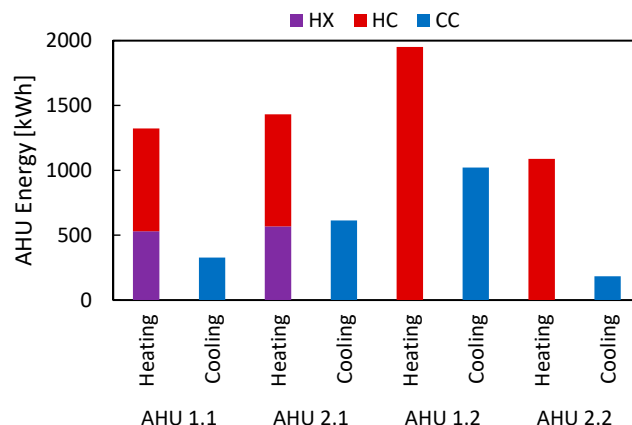


**Figure 15.** Total heating and cooling energy consumption of each AHU for the selected 24 h period.

## 5. Validating Simulation Models

The total heating and cooling energy demands in three different ice rink arenas with various AHUs are presented in Table 2. As shown, the energy demand results are provided from two different bases, one from the experimental measurements, and the other from the running simulations, and they are compared.

**Table 2.** The measurements and the simulation results of the three ice rink arenas.

Air Handling Units	AHU 2.2		AHU 1.1		AHU 2.1	
Temp. gradients	1.5 °C/m		1.6 °C/m		2 °C/m	
Measurements date&time	2016-05-20T14:55–2016-05-27T10:00		2016-05-03T10:50–2016-05-12T9:00		2016-06-15T14:50–2016-06-21T10:20	
-	Heating	Cooling	Heating	Cooling	Heating	Cooling
Measurement result	C: Mäntsälä		B: Klaukkala		A: Tapiola	
	9808 MWh	3755 MWh	8592.8 MWh	2907.6 MWh	10,695.5 MWh	4939.78 MWh
Simulation result	9485 MWh	3843 MWh	8731 MWh	2864 MWh	10,214 MWh	5179 MWh
Deviation	3.3%	2.3%	1.6%	1.5%	4.5%	4.8%

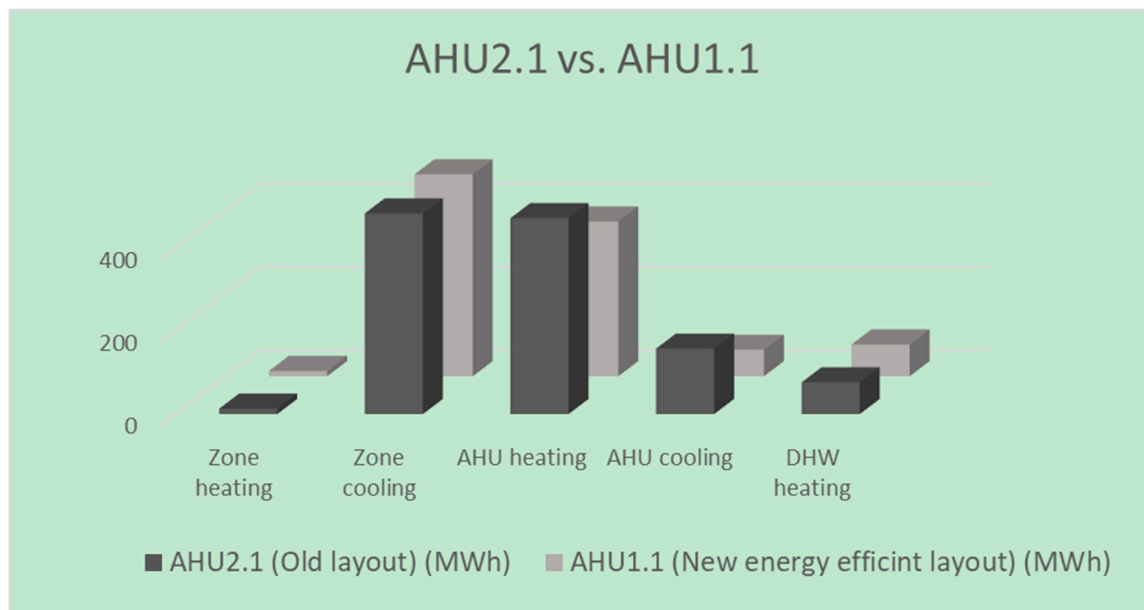
The measurements performed during May and June and the simulations correspondingly ran for similar periods of time. The simulations were carried out while the AHU layouts, building specification as well as control strategies similar as the measurements, were used. The simulation results, compared to the measurement results showed that the simulation models nearly always corresponded with the real measurements with less than 5% fault, as presented in Table 2. Therefore, the simulation models were verified to represent the energy demand behaviors of the ice rink arenas with an acceptable range of accuracy. The reason for such models is because it is not easy to measure the yearly energy demands of ice rinks, particularly with the variety of AHU layouts or various temperature gradients, which were required for this study. Therefore, it is necessary to validate the simulation models according to the measurements, and then run the simulation models for the entire yearly period, to obtain the results for various combinations.

## 6. Simulation Results

The heat exchanger and the cooling coil energy demands were independently studied, in order to highlight the significance of the AHU configurations. Table 3 and Figure 16 present heating and cooling energy demands by using two different AHU layouts, to clarify the impact of the AHU layouts on energy consumption. The simulation results of the AHUs indicate that approximately a reduction of 60% for cooling energy demands and a reduction of 21% for heating energy demands can be achieved by precisely planning the AHU layout.

**Table 3.** The yearly energy consumption results of the simulation for AHU1.1 and AHU2.1.

kWh	AHU2.1 (Old Layout) kWh/(m <sup>2</sup> a)	AHU1.1 (Energy-Efficient Layout) kWh/(m <sup>2</sup> a)	Reduced Energy %
Zone heating	5.6	5.6	−1.2%
Zone cooling	212.6	214.0	0
AHU heating	207.6	164.0	−21%
AHU cooling	69.3	28.1	−59.5%
DHW heating	33.6	33.6	0
Total	523.1	445.2	-

**Figure 16.** Comparison of cooling and heating energy demands between AHU2.1 and AHU1.1.

The simulation results of the cooling and heating energy demands are presented in Table 4 and Figure 17, while various temperature gradients have been applied, in order to study the impacts of temperature gradients on energy consumption.

**Table 4.** Simulation results of the yearly energy consumption of ice rinks with different temperature gradients.

Temperature Stratifications	Temperature Stratification 2 (°C/m)	Temperature Stratification 1.5 (°C/m)	Reduction	Temperature Stratification 1 (°C/m)	Reduction
Annual Energy consumption	kWh/(m <sup>2</sup> a)	kWh/(m <sup>2</sup> a)	%	kWh/(m <sup>2</sup> a)	%
Zone heating	10.2	7.4	27	7.9	−22
AHU heating	227.1	208.1	8	185.7	18
Zone cooling	274.6	179.8	35	170.0	38
AHU cooling	34.3	29.3	15	26.1	24
Electricity consumption of refrigeration plant	93.0	61.7	34	57.9	38
Condenser heat	367.7	241.5	34	227.9	38
In the case of using 50% of the condenser heat	183.8	120.7	34	113.9	38

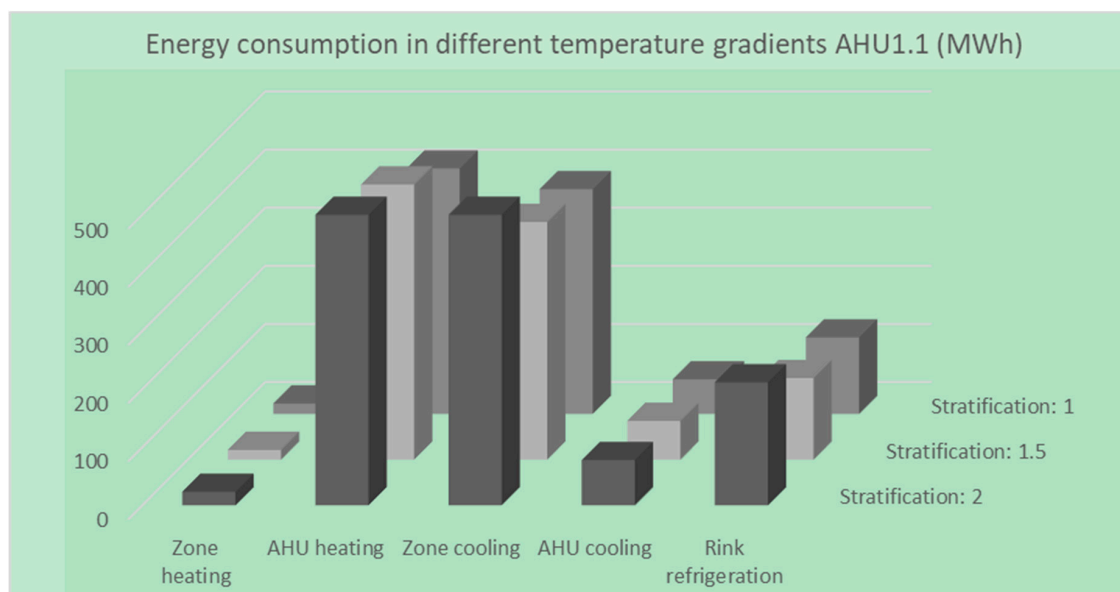


**Figure 17.** Energy consumption of different temperature gradients, AHU1.1.

There were three temperature gradient values, 2, 1.6, and 1.5 °C/m, measured on the three ice rinks, in which two of them were selected to be used in the simulation as high (2) and medium (1.5) temperature gradient values. The models were also simulated with an additional temperature gradient value equal to one, as an ultimate ideal condition.

Some of the measured cases included two supply air temperatures, warm and cool supply. However, this was instead simulated by using an average supply air temperature. The temperature gradient parameter in the building component takes in to account the effects of different air distribution solutions that create various temperature gradients in the simulation.

As presented in the Table 4, the energy demands for AHU cooling and AHU heating were decreased by 24% and 18%, respectively. The zone cooling of the ice-pad, as well as the electricity consumption requirements of the refrigeration process were both reduced by 38%. Finally, the overall results demonstrated clearly and concisely how energy can be significantly saved through re-planning the AHU layout and by reducing the indoor vertical temperature gradient.

## 7. Discussion

The most crucial challenge was how to implement the air distribution system in order to form a less stratified indoor air temperature. The ideal condition is to approach a temperature gradient of 1 °C/m. To do so, creating two thermally separated virtual zones should be considered. This means that two different temperatures are maintained in two warmer and cooler zones. The warmer zone is for the spectators, and the cooler zone is for the players. Therefore, it is reasonable to supply a more customized and localized air conditions to each zone, and then extract them from the same zone.

Figure 18 illustrates the air distribution strategies proposed by this study. As shown, the warmer air is supplied into the spectators' zone, and the cooler air into the players' zone. The air is extracted from the same zones similarly. The supply air terminals have to be as close to the occupants of the zones as possible. Two virtually separated zones are then created and subsequently, two different average temperatures are formed in each zone. The air distribution solutions reduce the risk of mixing the air within the zones. The virtual zones are indicated via dashed line boxes in the proposed air distribution models shown in Figure 18. As discussed earlier, such air distribution models more likely tend to approach the ideal temperature gradient of 1 °C/m on average. This study also verified that the lower temperature gradient results in lower cooling and heating energy demands, leading to more efficient planning of the AHU and air distribution systems. This is done by planning two separate

supply and exhaust ducts, to avoid the mixing of warmer and cooler air in the main ducts. Therefore, the cooler air may not need to go through the heating coil. Moreover, it justifies the planning of two completely separate AHUs, one for the player's zone, and the other for the spectator's zone. A further advantage of this solution is that the spectators' AHU does not need to run continuously. It may run conditional to the spectators' presence, with the speed control being proportional to the number of spectators.

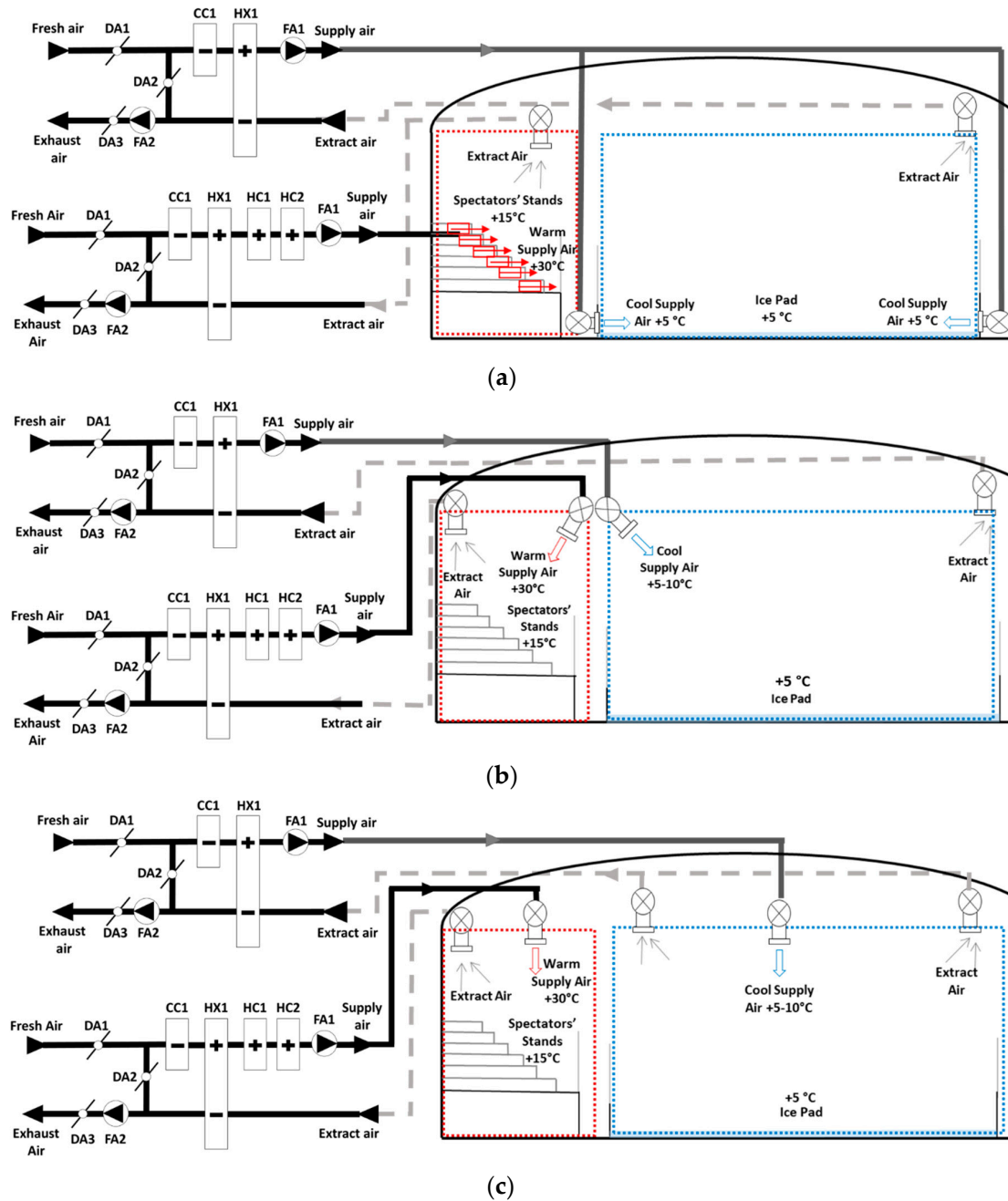


**Figure 18.** Proposed air distribution strategies to reduce the indoor temperature gradient. (a) Horizontal supply air; (b) inclined supply air; (c) vertical supply air.

## 8. Conclusions

This study points out the feasibility of reducing the heating energy required for space heating by approximately 21%, and reducing the cooling energy demand for dehumidification by about 60%. These results are achieved by carefully designing the AHU layouts. Furthermore, the more significant

result of the study are the impacts of indoor air temperature gradients on energy demand. Both the simulation and measurement results verify that the smaller the temperature gradient, the lower heating and cooling energy demands. The results indicate that the cooling power required for refrigeration process can be reduced by up to 38% by reducing the indoor temperature stratification from 2 °C/m to nearly 1 °C/m.

Considering the aforementioned conclusion necessitates careful design for both AHU configurations and air distributions. There are no precise air distribution models for creating any specific indoor air temperature gradient. However, as in the earlier examples proposed in Figure 18, more customized air distribution models tend to be more likely to reduce indoor air temperature gradient and this consequently leads to a more energy efficient system of air distribution. To do so, the heights and the directions of the airflows have to be more carefully planned, so that the heated or non-heated air is delivered right to the occupied zone where it is needed.

Finally, for the sake of energy conservation, it is proposed that common AHUs should not be planned for the entire arena. Instead, it is more intelligent to plan various AHUs for the spectator's zone and the rink zone, so that each AHU circulates air within its own thermal zone. The supply and exhaust air terminals have to be vertically placed in such a position as to prevent mixing of the warmer and the cooler air within the zones. If mixing of cooler and warmer air is avoided, then supplying additional heating will subsequently be avoided. The additional advantages of such a system are the control of the utilization of the spectator's AHU or its running speed based on the occupancy percentage in the spectator's zone.

**Author Contributions:** Conceptualization, methodology, data curation, software, visualization and writing—original draft preparation S.T., L.L. and M.T.; Validation, formal analysis and writing—review & editing M.T.; Supervision, project administration and funding acquisition, J.K.

**Funding:** This study was financed and supported by the Finnish Ministry of Education and Culture, through the (OKM) project, and by the Estonian Centre of Excellence in Zero Energy and Resource Efficient Smart Buildings and Districts, ZEBE, grant 2014-2020.4.01.15-0016 funded by the European Regional Development Fund.

**Conflicts of Interest:** The authors declare no conflict of interest.

## References

1. Pisello, A.L.; Bobker, M.; Cotana, F. A building energy efficiency optimization method by evaluating the effective thermal zones occupancy. *Energies* **2012**, *5*, 5257–5278. [CrossRef]
2. Domínguez, S.; Sendra, J.J.; León, A.L.; Esquivias, P.M. Towards energy demand reduction in social housing buildings: Envelope system optimization strategies. *Energies* **2012**, *5*, 2263–2287. [CrossRef]
3. Laurier Nichols, P. *Improving Efficiency in Ice Hockey Arenas*. ASHRAE Journal, USA. June 2009. Available online: <https://www.stantec.com/content/dam/stantec/files/PDFAssets/2017/Improving%20Efficiency%20in%20Ice%20Hockey%20Arenas.pdf> (accessed on 20 February 2019).
4. Rogstam, J.; Dahlberg, M.; Hjert, J. *Stoppsladd fas 3-Energianvändning i svenska ishallar; En studie av Svenska Ishallar i syfte att Främja Teknikutveckling och Hållbar Energianvändning*; Energy Kylanal. svenska kyltekniska föreningen: Älvsjö, Sweden, 2012.
5. Rogstam, J.; Dahlberg, M.; Hjert, J. *Stoppsladd fas 2 Energianvändning i Svenska ishallar; En studie av Svenska Ishallar i syfte att Främja Teknikutveckling och Hållbar Energianvändning*; svenska kyltekniska föreningen: Stockholm, Sweden, 2011.
6. Rojas, G.; Grove-Smith, J. Improving Ventilation Efficiency for a Highly Energy Efficient Indoor Swimming Pool Using CFD Simulations. *Fluids* **2018**, *3*, 92. [CrossRef]
7. Daoud, A.; Galanis, N.; Bellache, O. Calculation of refrigeration loads by convection, radiation and condensation in ice rinks using a transient 3D zonal model. *Appl. Therm. Eng.* **2008**, *28*, 1782–1790. [CrossRef]
8. Seghouani, L.; Daoud, A.; Galanis, N. Prediction of yearly energy requirements of indoor ice rinks. *Energy Build.* **2009**, *41*, 500–511. [CrossRef]
9. Seghouani, L.; Daoud, A.; Galanis, N. Yearly simulation of the interaction between an ice rink and its refrigeration system: A case study. *Int. J. Refrig.* **2011**, *34*, 383–389. [CrossRef]



10. Daoud, A.; Galanis, N. Prediction of airflow patterns in a ventilated enclosure with zonal methods. *Appl. Energy* **2008**, *85*, 439–448. [[CrossRef](#)]
11. Omri, M.; Galanis, N. Prediction of 3D Airflow and Temperature Field in an Indoor Ice Rink with Radiant Heat Sources. *Build. Simul.* **2010**, *3*, 153–163. [[CrossRef](#)]
12. Lestinen, S.; Koskela, H.; Jokisalo, J.; Kilpeläinen, S.; Kosonen, R. The use of displacement and zoning ventilation in a multipurpose arena. *Int. J. Vent.* **2016**, *15*, 151–166. [[CrossRef](#)]
13. Omri, M.; Barrau, J.; Moreau, S.; Galanis, N. Three-Dimensional Transient Heat Transfer and Airflow in an Indoor Ice Rink with Radiant Heat Sources. *Build. Simul.* **2016**, *9*, 175–182. [[CrossRef](#)]
14. Toomla, S.; Lestinen, S.; Kilpeläinen, S.; Leppä, L.; Kosonen, R.; Kurnitski, J. Experimental investigation of air distribution and ventilation efficiency in an ice rink arena. *Int. J. Vent.* **2018**. [[CrossRef](#)]
15. Palmowska, A.; Lipska, B. Experimental study and numerical prediction of thermal and humidity conditions in the ventilated ice rink arena. *Build. Environ.* **2016**, *108*, 171–182. [[CrossRef](#)]
16. Pennanen, A.S.; Salonen, R.O.; Aim, S.; Jantunen, M.J.; Pasanen, P. Characterization of air quality problems in five Finnish indoor ice arenas. *J. Air Waste Manag. Assoc.* **1997**, *47*, 1079–1086. [[CrossRef](#)] [[PubMed](#)]
17. Ouzzane, M.; Zmeureanu, R.; Scott, J.; Sunyé, R.; Giguere, D.; Bellache, O. Cooling Load and Environmental Measurements in a Canadian Indoor Ice Rink. *ASHRAE Trans.* **2006**, *112*, 538–546.
18. Piché, O.; Galanis, N. Thermal and economic evaluation of heat recovery measures for indoor ice rinks. *Appl. Therm. Eng.* **2010**, *30*, 2103–2108. [[CrossRef](#)]



© 2019 by the authors. Licensee MDPI, Basel, Switzerland. This article is an open access article distributed under the terms and conditions of the Creative Commons Attribution (CC BY) license (<http://creativecommons.org/licenses/by/4.0/>).